A Switched-capacitor DC-DC Converter with Voltage Regulation for Photovoltaic Applications

Naser Vosoughi Kurdkandi[1], Alireza Eyvazizadeh Khosroshahi[1], Seyed Hossein Hosseini[1]

[1]Department of Computer and Electrical Engineering, University of Tabriz, Tabriz, Iran
naser.vosoughi@yahoo.com, a.e.khosroshahi@gmail.com, hosseini@tabrizu.ac.ir

Abstract

In this paper, a new dc-dc switched-capacitor converter with the potential of output voltage regulation is presented for photovoltaic applications. The proposed topology consists of an extended high voltage gain converter along with a buck converter. The extended high voltage gain converter is operated with a fixed conversion gain whereas the buck converter is controlled to do the maximum power point tracking (MPPT) which is an important advantage of proposed structure. The most important benefits of the proposed structure are approximately continuous input current, reduction of the number of power electronic switches and costs. A comparison with other similar structures is given to show the merits of the proposed topology. The operation of proposed converter is verified using experimental results.

I. Introduction

Demand for clean and sustainable energy sources has dramatically increased during the past few years with growing population and industrial development. Since long time ago, fossil fuels have served as the major source of generating electrical energy, environmental consequences of these resources have made it necessary to benefit from new energy sources such as wind and solar. Photovoltaic systems (PV) could act as suitable choice for alleviating the aforementioned problems regarding provision of the local electrical energy for consumers, thanks to their low current expenditure and absence of transmission losses [1-4]. Output voltages of the PV modules are variable because of changes of temperature and sunlight. As a result, the low variable voltage of these clean energy technologies requires high voltage gain dc-dc converters with capability of MPPT tracking.

Small size, light weight, high power density, high efficiency, and most of all magnetic-less structure of switched-capacitor (SC) dc-dc converters have absorbed the attention of power engineers in the last years. Even in light load conditions high efficiency can be achieved [5]. These advantages have made SC dc-dc converters appropriate for application in battery powered systems and portable devices such as digital cameras and MP3 players [6]. As a result, many SC based dc-dc converters have been developed and proposed in previous studies [7-9]. However, SC dc-dc converters cannot be used for PV applications since they have a fixed voltage gain and cannot track the Maximum Power Point (MPP). In addition, their input current is not continuous.

Recently, several voltage multiplier converter topologies have been presented in [10-12]. A new voltage multiplier converter topology has been proposed in [10] which has been named multilevel flying-capacitor DC-DC converter. This topology consists of *n* capacitors and *2n* power switches. The value of generated DC voltage at output voltage for a special input voltage (V_{in}) is nV_{in}. It is clear that the number of utilized power switches will be increased to produce high voltage at output. Also, the value of output voltage is constant and cannot be regulated.

Another new voltage multiplier topology has been presented in [11]. In this topology, the number of used switches for *n* capacitors is *3n*. Then, the magnitude of output voltage will be $(n+1)V_{in}$ which is a constant value. Moreover, a new voltage multiplier structure has been introduced in [12] which need *n* capacitors and *2n* switches to produce nV_{in} at output. It is important to note that the input current of presented topologies in [10-12] is discontinuous and it is a restriction. Also, the voltage gain of these topologies is fixed and cannot be regulated. Therefore, these topologies cannot be utilized in PV systems because of their limitation to track the maximum power point.

In this paper, a new SC based converter for photovoltaic applications is proposed which can track the MPP and regulate its output voltage. Analysis and experimental results are added to confirm the performance and operation of proposed converter.

II. Proposed Switched Capacitor Converter

Fig. 1 shows the presented SC converter structure. This structure consists of two stages. The first stage is high voltage gain SC converter and the second stage is a buck converter. The SC stage consists of *n* charging capacitors, 2*n* switches, *n* power diodes and a dc voltage source. The elements of the buck converter are an inductor, a capacitor, a diode, and one switch.

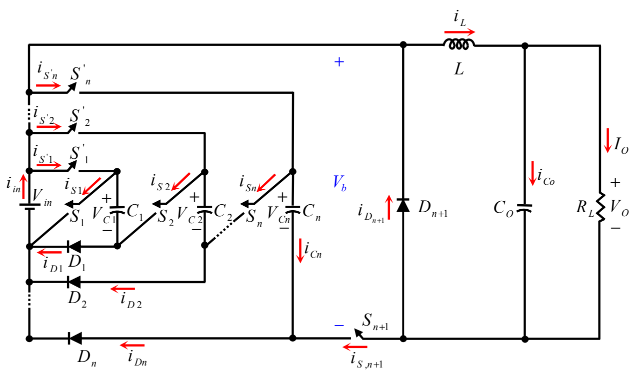

Fig. 1. The proposed SC based converter topology

The main disadvantages of the buck converter are:

- The input current is discontinuous.
- Voltage gain is limited and step-down.

Also, the major drawbacks of conventional SC converters are:

- Voltage regulation of output voltage is impossible.
- The input current is discontinuous.
- MPP tracking is not available.

So, to overcome the aforementioned limitations and disadvantages, the proposed converter can be an important structure. The main advantages of the proposed topology are as follows:

1) The input current of this structure is approximately continuous.

2) The voltage regulation of output voltage can be done by controlling the duty cycle of the buck converter.

3) The voltage gain can be step-down or step-up.
4) The proposed converter can track the MPP easily.
5) The number of used power electronic switches is low which leads to the reduction of costs.

All above mentioned advantages are verified by experimental and comparison results in the next sections. To explain the performance of proposed structure, the operation modes are described.

III. Operating Modes of The Proposed Structure.

Generally, there are two operating modes for the proposed topology as follows:

1) First operating mode (0<t<DT):

In this mode, the switches S_k, (k=1, …, $n+1$) are turned on. All diodes in the circuit structure are reverse biased and turned off. The inductor is charged linearly by the capacitors and the input voltage. Also, the output capacitor discharges to load. In this mode we have $V_b = (n+1)V_{in}$ where n is the number of charging capacitors. This mode is illustrated in Fig. 2(a).

2) Second operating mode (DT <t<T):

In this mode, the charging switches (S_k) are turned off and the complementary switches S'_j, (j=1, …, n) are turned on. In this mode, all diodes are forward biased and turned on. So, all SCs are in parallel with the input power source. Therefore, all SCs charge to the input voltage. Also, the inductor is discharged linearly by the output capacitor. This mode is shown in Fig. 2(b).

IV. Calculation of Proposed Converter Parameters

To obtain relationships for the most important parameters of proposed structure, the shown modes in fig. 2 are considered. The voltage gain and the values of elements such as inductors and capacitors are calculated for the proposed structure in this section.

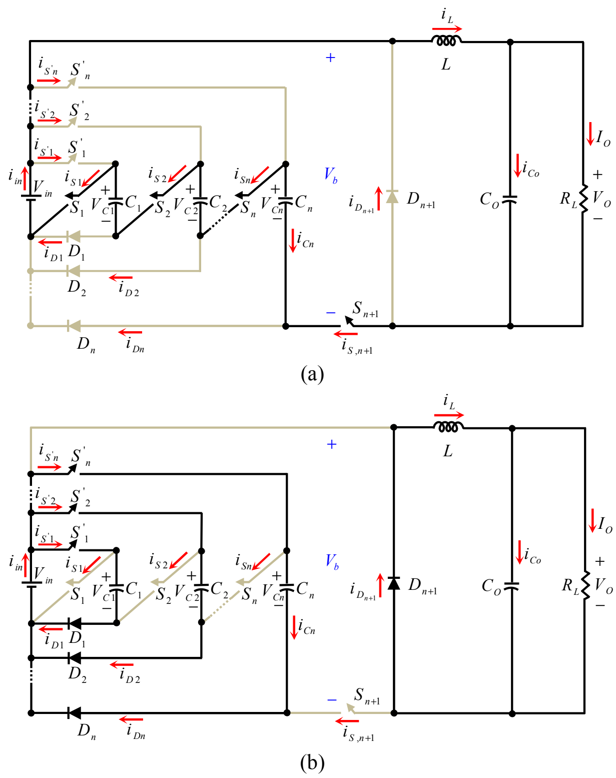

Fig. 2. Switching states of the proposed converter: (a) First operating mode, (b) Second operating mode

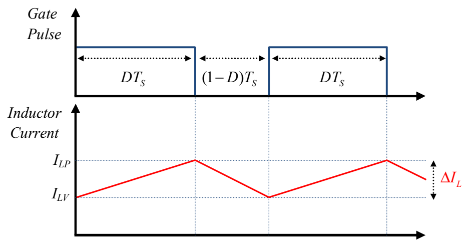

Fig. 3. Inductor current waveform

A. Calculation of voltage gain:

By applying the voltage-second balance principle to the inductor, the following equations are given:

$$\int_0^T V_L dt = \int_0^{DT} (\mathrm{V}_b - \mathrm{V}_o) dt + \int_{DT}^{T} -\mathrm{V}_o\, dt = 0 \tag{1}$$

Substituting V_b and solving (1), the voltage gain is obtained as:

$$M = \frac{V_o}{V_{in}} = (n+1)D \tag{2}$$

According to (2), by means of duty cycle D, the output voltage can be controlled in a wide range.

B. Current ripple and inductor value calculation

The inductor current is shown in Fig. 3 where the minimum and maximum value of the inductor current are indicated by I_{LV} and I_{LP}, respectively.

The inductor current is expressed by:

$$i_L(t) = \frac{1}{L}\int_0^t V_L dt + I_{LV} \qquad (3)$$

According to Fig. 3 and equation (3) we have:

$$I_{LP} = i_L(DT) = \frac{1}{L}\int_0^{DT} (V_b - V_o)dt + I_{LV} = \frac{D(V_b - V_o)}{fL} + I_{LV} \qquad (4)$$

So, the current ripple is calculated as:

$$\Delta I_L = I_{LP} - I_{LV} = \frac{[(n+1)V_{in} - V_o]D}{fL} \qquad (5)$$

From (2), the duty cycle is obtained as

$$D = \frac{V_o}{(n+1)V_{in}} \qquad (6)$$

Substituting (6) in (5), the value of inductor can be obtained as

$$L = \frac{(n+1)V_{in}V_o - V_o^2}{f\Delta I_L (n+1)V_{in}} \qquad (7)$$

C. Capacitance calculation of SCs

In the first operating mode, the SCs are in series with each other and the same current flows through each capacitor. In the second operating mode, the capacitors are charged in parallel and have the same voltage. As a result, the SCs can have the same capacitance $(C_1 = ... = C_n = C)$. The voltage of capacitor C_j (j=1, …, n) is expressed by

$$V_{C_j} = V_C = \frac{1}{C}\int_0^t i_C dt + V_C(0) \qquad (8)$$

According to (8), the voltage of capacitors at time $t=DT$ is

$$V_C(DT) = \frac{1}{C}\int_0^{DT} -I_o dt + V_C(0) = \frac{-I_o D}{fC} + V_C(0) \qquad (9)$$

where I_o is the output current defined as the ratio of output voltage to the output load (V_o/R_L). The voltage ripple across the SCs is defined as

$$\Delta V_C = V_C(0) - V_C(DT) = \frac{I_o D}{fC} \qquad (10)$$

Substituting D and I_o in (10), the capacitance of SCs is obtained as

$$C = \frac{V_o^2}{(n+1)V_{in}R_L f \Delta V_C} \qquad (11)$$

D. Capacitance calculation of output capacitor

As it is investigated in [13], the average current which flows through the output capacitor in its charging period equals to $\Delta I_L/4$. Also, the charging period is $T/2$. Then, we have:

TABLE I

COMPARISON OF PROPOSED TOPOLOGY WITH OTHER SIMILAR STRUCTURES

Type of Topology	[10]	[11]	[12]	Proposed Topology
Input current	Discontinuous	Discontinuous	Discontinuous	approximately Continuous
The number of used Switches	*2n*	*3n*	*2n*	*2n+1*
Capability of MPPT regulation	NO	NO	NO	Yes
Output voltage	Constant	Constant	Constant	Variable
Output voltage gain	nV_{in}	$(n+1)V_{in}$	nV_{in}	$(n+1)DV_{in}$
The number of charging capacitors	*n+1*	*n*	*n+1*	*n*

$$V_{C_o}(\mathrm{T}/2) = \frac{1}{C_o}\int_0^{T/2} \frac{\Delta I_L}{4} dt + V_{C_o}(0) \qquad (12)$$

So, the output capacitor ripple is expressed as

$$\Delta V_{C_o} = \frac{\Delta I_L}{8fC_o} \qquad (13)$$

Substituting (5) and (6) in (13), the capacitance of the output capacitor is calculated as

$$C_o = \frac{(n+1)V_{in}V_o - V_o^2}{8f^2 L \Delta V_{C_o}(n+1)V_{in}} \qquad (14)$$

V. ADVANTAGES OF THE PROPOSED STRUCTURE IN COMPARISON WITH OTHER SC CONVERTERS

To show the advantages of the proposed converter in comparison with other presented SC structures in [10-12], the comparison studies are provided in Table I. This comparison proves that the proposed structure is much better than other ones and it can be used in photovoltaic applications considering capability of MPPT.

When the converter is operating in the first mode, the inductor is charged by input source and when the converter is operating in the second mode the capacitors are charged by the input source. Then, in both of the operating modes the converters draws current from the input source. Based on this comparison, it is obvious that the input current of presented structure is approximately continuous. However, the input current of other structures are discontinuous.

Also, output voltage regulation capability is a significant advantage which only the proposed converter can set the output voltage using duty cycle of switches at each voltage level and tracking MPP of PV panels. This benefit makes the proposed converter appropriate for PV applications.

Also, the number of used charging capacitors is less than the structures proposed in [10] and [12].

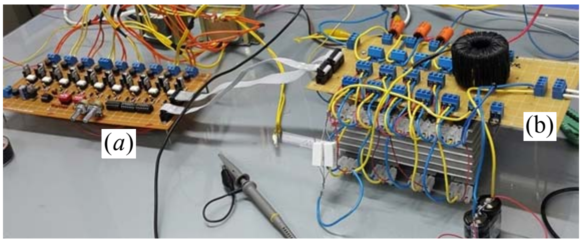

Fig. 4. Laboratory prototype and experimental setup, (a) switching control board and gate driver circuit, (b) power board

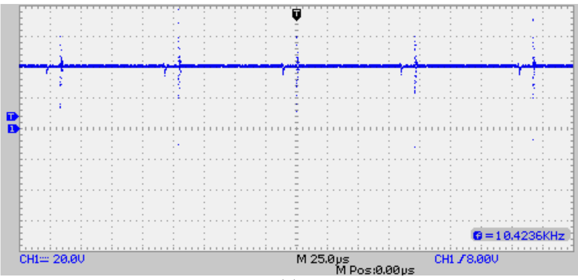

(a)

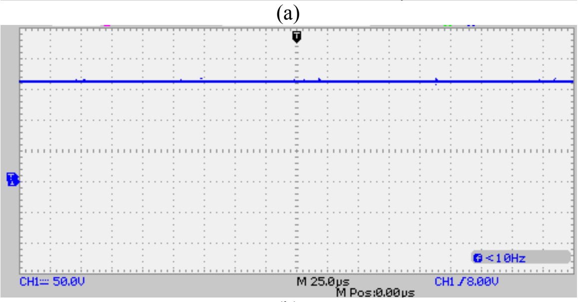

(b)

Fig. 5. The experimental result for (a) input voltage (b) output voltage

TABLE II

MAGNITUDES OF THE ELEMENTS OF PROPOSED TOPOLOGY

Parameter	Value/Number
Charging Capacitors	22 μF
L	7.7 mH
C_O	10 μF
Switching Frequency	10KHz
Load R_L	459.61 Ω
Power MOSFET	IRFP460
Diodes	MUR1560

All these comparison parameters in terms of used elements, voltage rating of the switches, cost and capability for PV applications prove the merits of suggested converter in comparison with other structures.

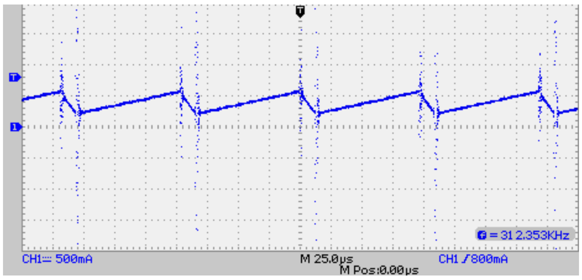

Fig. 6. The inductor current

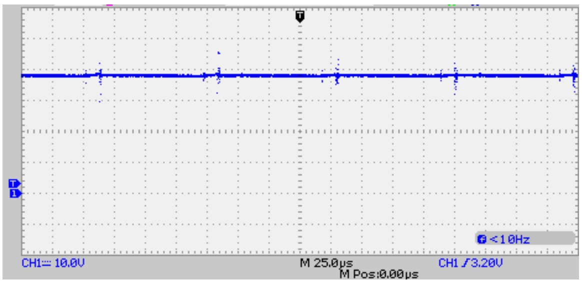

Fig. 7. Experimental results for voltage across of C_2

VI. EXPERIMENTAL RESULTS

To verify the operation of the proposed converter, the structure has been built up in a laboratory scale for *n*=4. The prototype and experimental setup is indicated in Fig. 4.

The manufacturer numbers of MOSFETs, power diodes and magnitudes of employed elements and parameters for the proposed structure are given in table II. These values are designed according to the equations given in section IV.

Fig. 5 shows the experimental result for the input and output voltages. As shown in this figure, the input voltage of 40 V is boosted to 165 V in the output. Also, it can be seen that with a small capacitance (*10 μF*), the output voltage ripple is low.

The inductor current waveform is indicated in Fig. 6.

Fig. 7 shows the voltage across a typical capacitor. The voltage across of other charging capacitors is similar with the voltage across C_z.

Fig. 8 shows the typical blocked voltage by the switches. These waveforms determine the voltage rating of the switches. Fig. 7(a) indicates the blocked voltage by the switch S_1. It is noticeable that this waveform is similar with the blocked voltage by the S_2, S_3 and S_4 switches. Fig. 7(b) indicates the blocked voltage by the complementary switch S'_1. Fig. 7(c) shows the blocked voltage by the switch S_5.

According to the experimental results, the average input current of the converter is 1.57 A and the input voltage is 40, therefore the input power is 62.8 W. The average output current of the converter is 0.36 A and the output voltage is 165 V. Then, the output power is 59.4 W. So, it is concluded that the efficiency of the converter is 94.58 %.

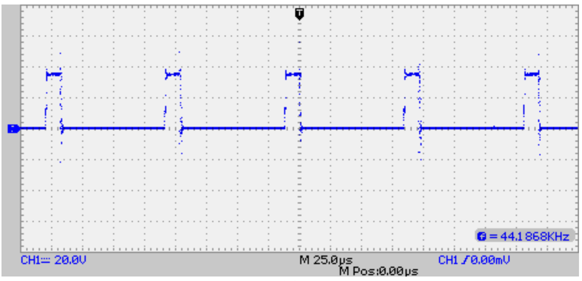

(a)

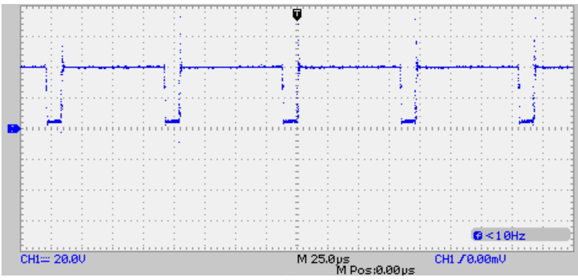

(b)

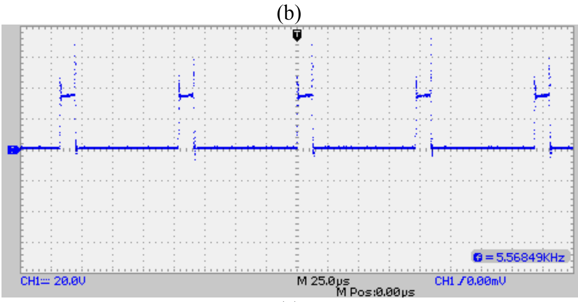

(c)

Fig. 8. The blocked voltage by the switch (a) S_1, (b) S'_1, (c) S_5.

VII. CONCLUSIONS

In this paper, a new switched-capacitor converter was presented for photovoltaic applications. Operating modes and mathematical analysis of the presented structure were analyzed. Using the proposed structure, the disadvantages of switched-capacitor converters was improved. Approximately continuous input current, higher voltage gain and better regulation of output voltage were the most important features of proposed topology. It was shown that the proposed topology is suitable for photovoltaic systems. Experimental works for the presented converter were presented to validate the features of it.

REFERENCES

[1] A. Ajami, H. Ardi, and A. Farakhor, “A Novel High Step-up DC/DC Converter Based on Integrating Coupled Inductor and Switched-Capacitor techniques for Renewable Energy Applications”, *IEEE Trans. On Power Electron.* vol.30, no.8 pp. 4255 – 4263, Aug. 2015.

[2] M.R. Banaei, H. Ardi, R. Alizadeh, and A. Farakhor, “Non-isolated multi-input–single-output DC/DC converter for photovoltaic power generation systems,” *IET Power Electron.*, vol. 7, no. 11, pp. 2806–2816, 2014.

[3] S.H. Hosseini, A. Farakhor, and S. Khadem Haghighian, “Novel Algorithm of MPPT for PV Array Based on Variable Step Newton-Raphson Method Through Model Predictive Control,” *In 13th Inter. Conf. on control, automation and systems*, 2013, pp. 1577 - 1582.

[4] A.E. Khosroshahi, M. Abapour, and M. Sabahi, “Reliability Evaluation of Conventional and Interleaved DC–DC Boost Converters,” *IEEE Trans. Power Electron.*, vol.30, no.10, pp. 5821-5828, Oct. 2015.

[5] M. S. Makowski, D. Maksimovic, “Performance limits of switched-capacitor DC-DC converters,” *in Proc. IEEE Power Electron. Spec. Conf.*, 1995, vol. 2, pp. 1215–1221.

[6] A. Ioinovici, “Switched-capacitor power electronics circuits,” *IEEE Circuits Syst. Mag.*, vol. 1, no. 3, pp. 37–42, Sep. 2001.

[7] H.S. Chung, A. Ioinovici, and C. Wai-Leung, “Generalized structure of bi-directional switched-capacitor DC/DC converters,” *IEEE Trans. Circuits Syst. I, Fundam. Theory Appl.*, vol. 50, no. 6, pp. 743–753, Jun. 2003.

[8] M. D. Seeman and S. R. Sanders, “Analysis and optimization of switched-capacitor DC-DC converters,” *IEEE Trans. Power Electron.*, vol. 23, no. 2, pp. 841–851, Mar. 2008.

[9] R. Jain, “A novel switched capacitor circuit for efficient voltage regulation,” *in Proc. 7th ICCDCS*, 2008, pp. 1–6.

[10] Zhang, Fan, Lei Du, Fang Zheng Peng, ZhaomingQian, "A new design method for high-power high-efficiency switched-capacitor dc–dc converters" *IEEE Transactions on Power Electronics*, vol. 23, no. 2, pp. 832-840, 2008.

[11] Pan, Zhiguo, Fan Zhang, and Fang Z. Peng, “Power losses and efficiency analysis of multilevel dc-dc converters,” *Applied Power Electronics Conference and Exposition*, vol. 3, 2005.

[12] Qian, Wei, et al, “A switched-capacitor DC–DC converter with high voltage gain and reduced component rating and count,”*IEEE Transactions on Ind. Applications*, vol. 48, no. 4, pp. 1397-1406, 2012.

[13] E. Babaei, M. E. Seyed Mahmoodieh, and M. Sabahi, “Investigating Buck DC-DC Converter Operation in Different Operational Modes and Obtaining the Minimum Output Voltage Ripple Considering Filter Size,” *Journal of Power Electron.* , vol. 11, no. 6, pp.793-800 , 2011.